ACS OMEGA

http://pubs.acs.org/journal/acsodf

Article

Design and Preparation Technology of Single/Dual-Cross-Linking Copolymers Based on *Swida wilsoniana* Oil

Ruitong Liu, Jing Yi, Shouhai Li,* Jianling Xia, Mei Li, Haiyang Ding, Lina Xu, Xiaohua Yang, and Na Yao

Cite This: *ACS Omega* 2021, 6, 21915−21924

Read Online

ACCESS | Metrics & More | Article Recommendations

ABSTRACT: To fully utilize the forestry bioresources, a novel dual-cross-linkable resin monomer of MAHSWAGMA was prepared from *Swida wilsoniana* oil (SWO). FT-IR and ^{1}H-NMR analysis demonstrated the successful synthesis of the target product. Five different cross-linking copolymers, including a polymerized vinyl ester/single-cross-linking (PVESC) polymer, a polymerized epoxy/single-cross-linking (PESC) copolymer, a thermal-photo-initiated/dual-cross-linking (TPIDC) copolymer, a photo-thermal-initiated/dual-cross-linking copolymer (PTIDC), and a thermal-initiated/dual-cross-linking copolymer (TIDC), were obtained with different preparation technologies by different initiated cross-linking processes. Thermal and mechanical properties of the five copolymers were all tested, and the effects of different preparation technologies on the properties of prepared copolymers were investigated. The prepared three dual-cross-linking copolymers had higher hardness, relative cross-linking density, glass transition temperature, and more excellent mechanical property than the other two single-cross-linking copolymers. The PTIDC copolymerized system obtained with photo first and thermal latter initiated dual-cross-linking preparation technology had the most excellent comprehensive properties. This study can provide an ideal idea for the design and preparation of dual-cross-linking copolymers based on forestry vegetable oil.

1. INTRODUCTION

Swida wilsoniana, a dicotyledon, is up to 40 m tall and has gray bark.[1−3] Owing to the strong adaptability, photophilia, and cold tolerance, *S. wilsoniana* can survive in alkaline, neutral, weakly alkaline, and mildly saline and alkaline lands.[4] It can be planted extensively not only in hills, plains, and mountains but also in ridges of fields, riversides, and houses both in the front and behind. *S. wilsoniana* is widely distributed in the subtropical and temperate zones of both hemispheres.[5,6] As a high oil yield plant, its flesh and kernel are enriched with 30% oil.[6] *S. wilsoniana* oil (SWO) contains up to 77% oleic and linoleic acid (Figure 1).[7,8] SWO containing many unsaturated double bonds is a novel functional high-quality woody vegetable oil that has higher molecular design ability and wider application prospects in chemical reactions.[9−11]

Generally, common synthetic polymers based on vegetable oil have excellent flexibility, but their further application is still restricted by some limitations, such as insufficient mechanical rigidity and easy deformation under heating.[12,13] Dual-cross-linking copolymers are a novel type of copolymerized systems based on the dual-cross-linking technology.[14] Usually, the resin monomers in a dual-cross-linking system are cross-linked through independent reaction stages by different reaction

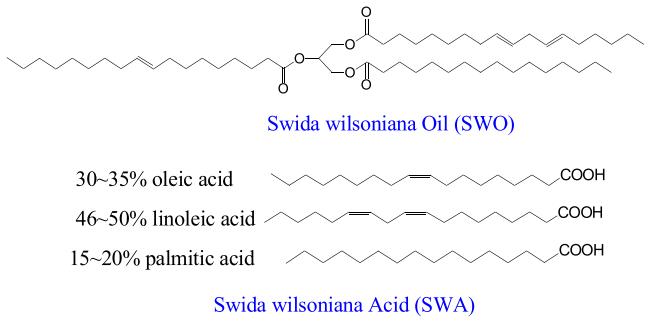

Figure 1. Formulas of *Swida wilsoniana* oil (SWO) and *Swida wilsoniana* acid (SWA).

principles,[15,16] such as microwave, thermal, room temperature, UV light, or moisture cross-linking.[17−20] Different from the

Received: April 26, 2021
Accepted: August 6, 2021
Published: August 19, 2021

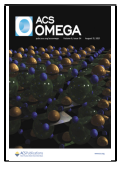

https://doi.org/10.1021/acsomega.1c02199
ACS Omega 2021, 6, 21915−21924

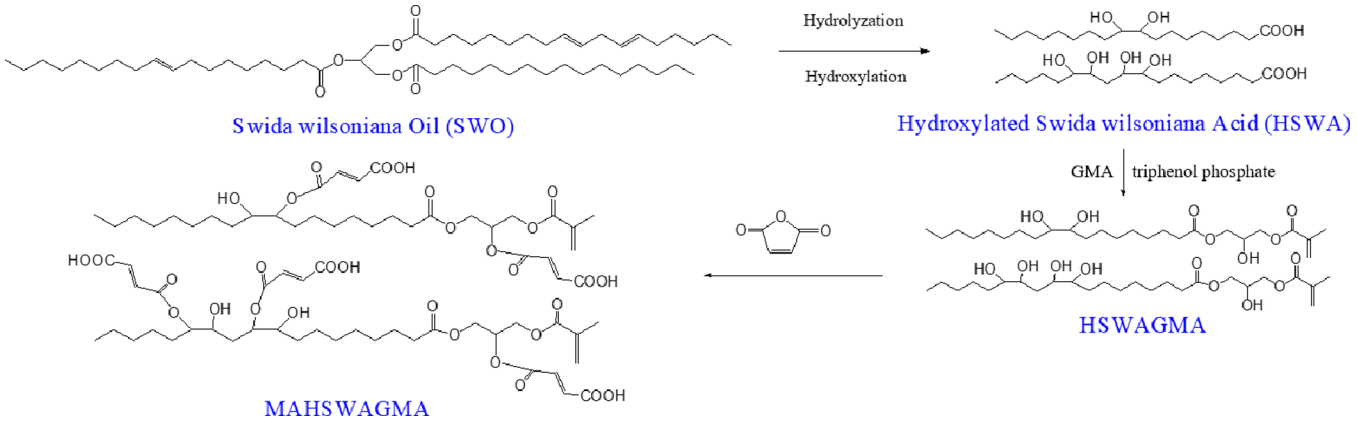

Figure 2. Synthetic route scheme of MAHSWAGMA.

single-cross-linking method, the dual-cross-linking technology can improve the application of superthick coatings, complicated shape products, opaque materials, and other materials. With diverse application prospects, the dual-cross-linking technology can be widely used not only in electronics, medicine, and construction but also in petrochemical, metallurgy, and other industries.[21−23] In addition, especially for the dual-cross-linking system, the different preparation technologies have a huge impact on the comprehensive properties of the prepared copolymers.[17−23]

With the emergence of environmental pollution and shortage of nonrenewable resources, the durability of materials and the awareness of environmental protection have been gradually aroused by researchers, promoting the research of biology-based dual-cross-linking copolymerized systems.[24−26] Woody vegetable oil is an important biomass forestry resource.[27,28] Abundant forestry resources are distributed worldwide, and the annual output of woody vegetable oil is more than 10 million tons.[29]

As we know, there have been few systematic research on *Swida wilsoniana* oil-based polymers with different initiated cross-linking processes in recent years. In this work, five different single-cross-linking and dual-cross-linking polymerizations have been designed according to different initiation cross-linking processes and different preparation technologies. The comprehensive properties of *Swida wilsonana* oil-based cross-linking polymers were systematically studied.

2. EXPERIMENTAL SECTION

2.1. Materials. SWO (46−50% linoleic acid, 30−35% oleic acid, and 15−20% palmitic acid; iodine value: 104−116.8 gI_2/100 g) was purchased from Jiangxi Fenglin Investment and Development Co., Ltd., China. Sodium hydroxide (98.0%), ethyl alcohol (99.0%), and formic acid (88.0%) (all stabilized) were purchased from Shanghai Lingfeng Chemical Reagent Co., Ltd., China. Hydrochloric acid (37%), ethyl acetate (99.5%), *P*-toluene sulfonic acid (98.5%), and H_2O_2 (30%) (all stabilized) were provided by Nanjing Chemical Reagent Co., Ltd., China. Maleic anhydride (99.5%), triphenyl phosphate (98.0%), 2,2-dimethoxy-2-phenylacetophenone (DMPA, 98%), and hydroquinone (99.0%) (all stabilized) were offered by Sinopharm Chemical Reagent Co., Ltd., China. E51 epoxy resin and tris (dimethylaminomethyl)phenol (DMP-30) were purchased from Wuxi resins Co., Ltd., China. Glycidyl methacrylate (GMA, stabilized, 97%) was produced by Aladdin Industrial Corporation (Shanghai). All these chemicals were used as received.

2.2. Preparation. *2.2.1. Preparation Process of Hydroxylated S. wilsoniana Acid (HSWA).* *S. wilsoniana* acid (SWA) can be prepared via hydrolyzation of SWO. NaOH (25.04 g) was first dissolved into 240 mL of 50 wt % ethanol water solution. The obtained solution was introduced into a four-necked flask and heated to 70 °C. Then, 150.00 g of SWO was added. The mixture was maintained at about 70 °C and kept for 2 h. HCl solution (5 mol/L) was added to adjust the pH of the mixture at 2−3 and then the acidification continued at 68−72 °C for 1 h. When the acidification was over, the supernatant SWA can be obtained after standing for 30−60 min. The obtained crude SWA product was then washed at least three times with distilled water. Next, the residual distilled water was removed via vacuum distillation. Finally, an orange colored viscous mixed fatty acid liquid named SWA was obtained (yield: 93.20%).

SWA (120.00 g), 1.52 g of *P*-toluene sulfonic acid, and 24.00 g of formic acid were added into a sizable flask. H_2O_2 (102.00 g) was slowly added at 50 °C. After this, the reaction was gradually heated to 65 °C and then kept reacting for 5 h. Subsequently, 25.00 g of H_2O and 50.00 g of ethyl acetate were added and kept for 2−5 min. The supernatant oil layer of crude HSWA can be obtained after standing for 30−60 min. The obtained crude HSWA product was then washed at least three times with distilled water. Next, ethyl acetate and the residual distilled water were all removed by vacuum distillation. Finally, a viscous liquid of HSWA was obtained (acid value: 192.54 mg (KOH)/g; hydroxyl value: 0.364 mol/100 g (yield: 86.06%)).

2.2.2. Preparation of SWO-Based Vinyl Resin Monomers. The SWO-based vinyl resin monomer can be obtained from HSWA. First, 0.40 g of triphenyl phosphate, 0.08 g of hydroquinone, and 78.38 g of HSWA were added in a four-necked flask. GMA (38.24 g) was then slowly added at 80 °C. After this, the mixture was stirred for 2 h at 118 °C. After the temperature of the mixture was dropped below 85 °C, 52.76 g of maleic anhydride (MA) was added, and the reaction was continued for 2 h. Finally, MA-modified HSWAGMA (MAHSWAGMA) was prepared (acid value: 139.57 mg (KOH)/g) (yield: 95.86%). The synthetic route of MAHSWAGMA is displayed in Figure 2.

2.2.3. Preparation Technology of Copolymers. Five copolymers, including a polymerized vinyl ester/single-cross-linking polymer (PVESC), a polymerized epoxy/single-cross-

https://doi.org/10.1021/acsomega.1c02199
ACS Omega 2021, 6, 21915−21924

linking copolymer (PESC), a thermal-photo-initiated/dual-cross-linking copolymer (TPIDC), a photo-thermal-initiated/dual-cross-linking copolymer (PTIDC), and a thermal-initiated/dual-cross-linking copolymer (TIDC), can be obtained with different initiating polymerization methods.

PVESC can be obtained by casting MAHSWAGMA and DMPA (the photoinitiator) into a polytetrafluoroethylene (PTFE) mold and curing with a UV-curing device (100 mw/cm^2) for 10 min. For PVESC, the polymerized system was formed by the radical polymerization among the double bonds of MAHSWAGMA under UV light irradiation.

PESC was synthesized by casting MAHSWAGMA, E51, and DMP-30 into a preheated PTFE mold. The mold was heated to 120 °C for 2 h. For PESC, the copolymerized system was formed via the reaction between the carboxyl groups of MAHSWAGMA and the epoxy groups of E51.

TPIDC was obtained by casting E51, MAHSWAGMA, DMP-30, and DMPA into a PTFE mold and curing under certain conditions. The mold was heated to 120 °C for 1 h and then further cured under UV light for another 10 min. For TPIDC, the carboxyl groups of MAHSWAGMA first reacted with the epoxy groups, and then, DMPA triggered the radical polymerization of C═C of MAHSWAGMA under UV light.

PTIDC was obtained by casting MAHSWAGMA, E51, DMP-30, and DMPA (the photoinitiator) into a plane PTFE mold curing under certain conditions. The mixture was first cured under UV light for 10 min and then was further cured at 120 °C for 1 h. For PTIDC, DMPA first triggered the radical polymerization of C═C of MAHSWAGMA under UV light, and then, the carboxyl groups of MAHSWAGMA further reacted with the epoxy groups of E51.

TIDC was produced by casting E51, DMP-30, MAHSWAGMA, and *tert*-butyl peroxybenzoate (the initiator) into a PTFE mold. The mixture was first heated to 120 °C for 2 h and then heated to 150 °C for 2 h. For TIDC, the radical polymerization of C═C and the reaction between the carboxyl groups and epoxy groups were all triggered simultaneously under the heating condition.

Table 1 shows the detailed data of the mixed systems, and Figures 3 and 4 display the reacting mechanisms of different cross-linking systems.

Table 1. Formulation of Different Copolymerized Systems

samples	MAHSWAGMA (g)	E51 (g)	DMP-30 (g)	DMPA (g)	*tert*-butyl peroxybenzoate (g)
PVESC	10.00	0.00	0.00	0.15	0.00
PESC	10.00	6.22	0.19	0.00	0.00
TPIDC	10.00	6.22	0.19	0.24	0.00
PTIDC	10.00	6.22	0.19	0.24	0.00
TIDC	10.00	6.22	0.19	0.00	0.16

2.3. Characterization. *2.3.1. Fourier Transform Infrared Spectroscopy (FT-IR) Analysis.* A Nicolet iS10 FT-IR Spectrometer was used to acquire FT-IR spectra of different samples with the wavenumber ranging from 4000 to 500 cm^{-1}.

2.3.2. ^{1}H-Nuclear Magnetic Resonance (NMR) Analysis. An ARX-300 nuclear magnetic resonance spectrometer (Bruker, Switzerland) was used to record ^{1}H-NMR (300 MHz) spectra, and $CDCl_3$ was employed as a deuterated solvent.

2.3.3. Tensile Property Analysis of Different Copolymers. Tensile properties of all copolymers were tested with a universal testing machine (CMT4303, SANS, USA) at 25 °C. Tensile specimens were cured in dumbbell-shaped molds, in accordance with ASTM D638-03. For each sample, five specimens with a size of 100 × 10 × 5 mm^3 were tested at room temperature for average values. The testing speed is 10 mm/min.

2.3.4. Hardness Analysis of Different Copolymers. A Shore D durometer (TH210, TIME, China) was used to test the hardness of different specimens at room temperature.

2.3.5. Microstructure Analysis of Copolymers. The tensile fracture surface of the samples was treated with golden powder, and then, a scanning electron microscopy meter (S-3400N, Hitachi, Japan) was used to obtain micrographs by magnifying 500 times.

2.3.6. Dynamic Mechanical Thermal Analysis (DMA) of Copolymers. A dynamic mechanical thermal analyzer (Q800, TA, USA) was applied to test dynamic mechanical thermal properties with the tensile test method. The specimens (50 × 5 × 2 mm^3) were tested at a heating rate of 3 °C/min from −60 to 150 °C with a frequency of 1 Hz.

2.3.7. Thermogravimetric Analysis (TGA) of Copolymers. A thermogravimetric analysis device (ST A409PC, NETZSCH, Germany) was used to test the thermal stability of copolymers. The specimens were heated from 25 to 800 °C under a nitrogen atmosphere at a heating rate of 20 °C/min. Generally, 10−14 mg samples were used for the test.

3. RESULTS AND DISCUSSION

3.1. FT-IR Analysis of Monomers. FI-IR spectra of SWO, HSWA, HSWAGMA, and MAHSWAGMA are shown in Figure 5. SWO shows a strong IR absorption peak (1743 cm^{-1}) corresponding to the ester group. Meanwhile, the signals of C−O−C at 1161 and 1097 cm^{-1} further proved the presence of the ester group. The peaks at 721 and 3007 cm^{-1} represent the vibration of C−H in the vinyl group. In addition, the weak peak at 1639 cm^{-1} represented the bending vibration of carbon−carbon double bonds. These three peaks confirmed the presence of the vinyl group on the alkyl chain of SWO.

The spectrum of HSWA shows the peaks at 910 and 1376 cm^{-1} corresponding to the bending vibration of O−H in the carboxyl group. The broad weak peak at 2400−3400 cm^{-1} is assigned to the carboxyl groups of HSWA in the associating state. In addition, it can be observed that the peaks at 1161 and 1639 cm^{-1} corresponding to the carbon−carbon double bonds and ester groups, respectively, ever displayed in the FT-IR spectrum of SWO were all disappeared. These changes indicate that HSWA has been synthesized successfully.

For the spectrum of HSWAGMA, the intensity of the peak at 3431 cm^{-1} is obviously stronger than that in the HSWA spectra, which indicates that the hydroxyl content of HSWAGMA is higher than that of HSWA. Meanwhile, the ester absorption peak can be clearly identified at 1718 cm^{-1}. The shift of the peak is related to the conjugation of the double bond with the carbonyl group. The absorption peaks at 1162 and 1295 cm^{-1} correspond to the symmetric and asymmetric stretching vibration of C−O−C in the ester group, respectively. In addition, the absorption peak of the vibration of carbon−carbon double bonds at 1637 cm^{-1} shifted to low frequency due to the existence of conjugate structures. Compared with the FT-IR spectrum of HSWA, the peak at 2400−3400 cm^{-1} corresponding to the carboxyl group

https://doi.org/10.1021/acsomega.1c02199
ACS Omega 2021, 6, 21915−21924

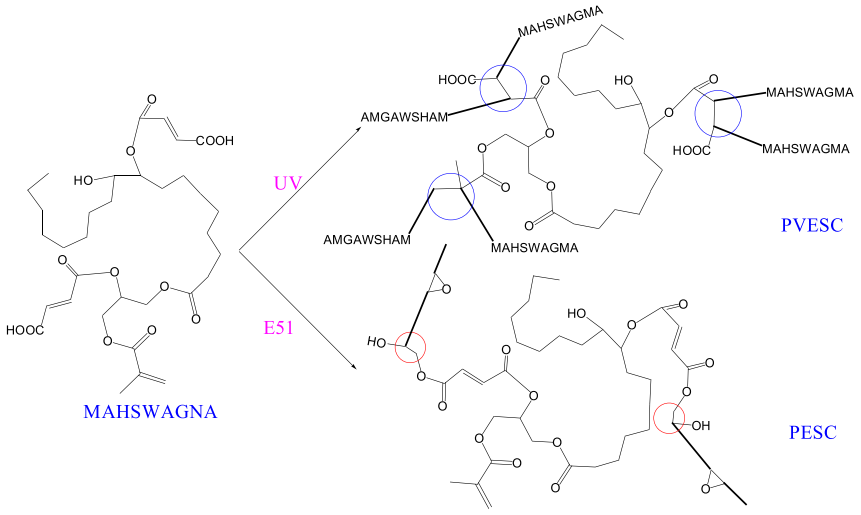

Figure 3. Preparation mechanisms of two single-cross-linking systems.

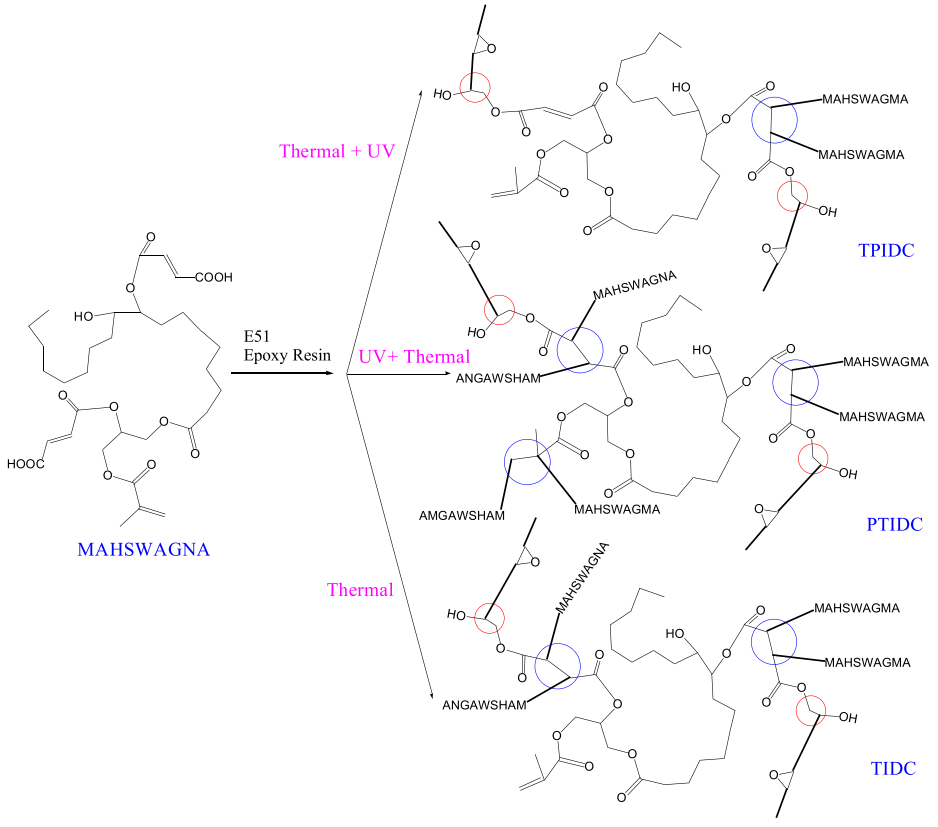

Figure 4. Preparation mechanisms of three dual-cross-linking systems.

disappeared, which further indicates the successful preparation of HSWAGMA.

For the FT-IR spectrum of MAHSWAGMA, compared with the spectra of HSWAGMA, the intensity of the absorption peak at about 1641 cm^{-1} of C═C and the stretching peak at about 1720 cm^{-1} of carbonyl groups on the spectrum of MAHSWAGMA were all increased obviously. Moreover, the disappearance of the peak at about 3498 cm^{-1}(corresponding to the hydroxyl group) and the appearance of the peak ranging from 2400 to 3400 cm^{-1} (corresponding to the carboxyl groups) further indicate that MAHSWAGMA has been successfully synthesized.

3.2. ^{1}H-NMR Analysis. Figure 6 displays the ^{1}H-NMR spectra of SWO, HSWA, HSWAGMA, and MAHSWAGMA. For the ^{1}H-NMR spectrum of SWO, the peaks at 5.3, 4.1, 2.3, and 2.0 ppm are assigned to the protons on double bonds, on carbon atoms adjacent to hydroxyl groups, and on carbon atoms adjacent to carbonyl groups and on hydroxyl groups. Compared to SWO, the ^{1}H-NMR spectrum of HWSA displays resonances at 1.9−0.8 ppm stemming from the methyl and methylene protons of HSWA, indicating that HSWA has been successfully synthesized. As for HSWAGMA, peaks at 4.3−3.9 correspond to the methylene protons next to oxygen atoms of the ester groups, and peaks at 4.5 and 3.8−3.5 correspond to

https://doi.org/10.1021/acsomega.1c02199
ACS Omega 2021, 6, 21915−21924

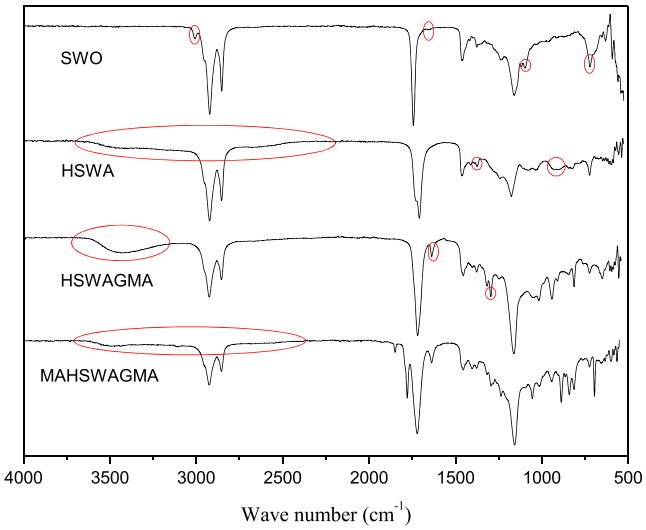

Figure 5. FT-IR spectra of SWO, HSWA, HSWAGMA, and MAHSWAGMA.

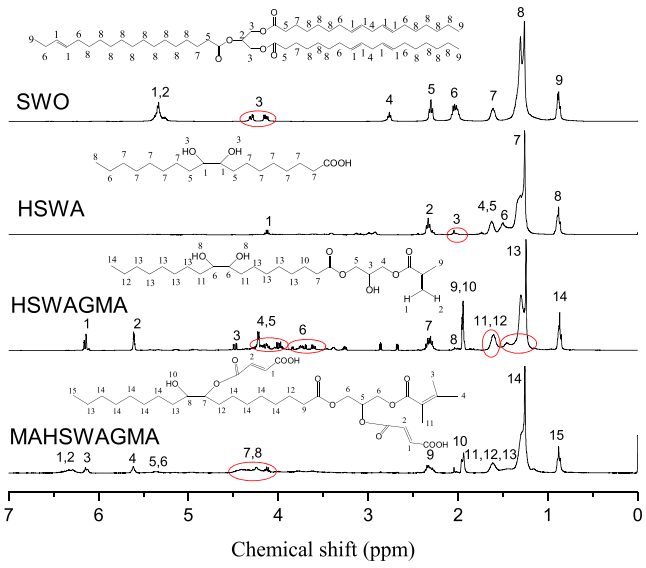

Figure 6. ^{1}H NMR spectrum of SWO, HSWA, HSWAGMA, and MAHSWAGMA.

the protons on the carbon atoms attached to the hydroxyl group. HSWAGMA displays two resonances at 6.2 and 5.6 ppm stemming from carbon−carbon double bonds of GMA. The peaks at 1.9−0.8 ppm are assigned to the methylene and methyl protons of HSWAGMA.

In MAHSWAGMA, the peaks at 3.8−3.5 and 4.5 ppm ascribed to carbon atom protons of the hydroxyl group were not observed. The MAHSWAGMA spectrum also shows the characteristic peaks at 6.3, 6.1, and 4.1−4.5 ppm corresponding to the protons on CH═CH of the maleic anhydride moiety and on carbon adjacent to oxygen atoms from the ester groups, respectively. These findings indicate that MAHSWAGMA has been successfully synthesized.

3.3. Hardness and Tensile Properties of Different Copolymerized Systems. The tensile stress−strain curves of PVESC, PESC, TPIDC, PTIDC, and TIDC are displayed in Figure 7, and the details are shown in Table 2. Both PVESC and PESC had low tensile strength (0.80 and 0.92 MPa) and high elongation at break (27.68 and 38.88%). The mechanical

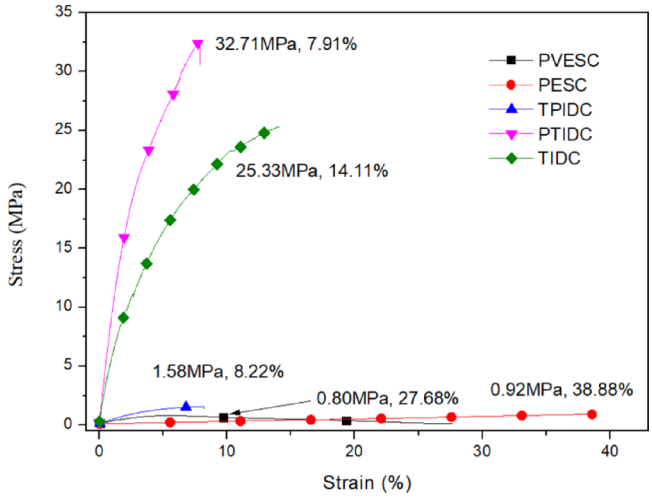

Figure 7. Tensile stress−strain curves of PVESC, PESC, TPIDC, PTIDC, and TIDC.

Table 2. Detailed Data of Mechanical Properties of Different Copolymers

samples	tensile strength (MPa)	elongation at break (%)	shore hardness (HD)
PVESC	0.80	27	40
PESC	0.92	38	38
TPIDC	1.58	8	45
PTIDC	32.71	7	68
TIDC	25.33	14	65

properties of polymers depend on the chemical structures and cross-linking state of copolymerized monomers (Figure 8). For the MAHSWAGMA monomer, it contains numerous flexible alkyl chains and two kinds of functional groups (including the double bond and the carboxyl group). In PVESC, the double bonds of MAHSWGMA were triggered by radical polymerization through UV light irradiation, while in PESC, the epoxy groups of E51 epoxy resin can react with the carboxyl groups of MAHSWAGMA at 120 °C. Although PVESC and PESC have some characters of tough materials, they still possess poor mechanical properties caused by the lower cross-linking density and limited functional groups.

TPIDC had low tensile strength (1.58 MPa) and low elongation at break (8.22%). Most of the molecular segments were fixed after curing at 120 °C for 1 h and consequently cannot move freely for further polymerization under UV light irradiation. Thus, the dual-cross-linking effect of TPIDC is not ideal, and the mechanical properties are poor. In the PTIDC system, DMPA triggered first the radical polymerization of the double bonds of MAHSWAGMA under UV light; meanwhile, the part of carboxyl groups might react with epoxy groups under the influence of thermal effect of UV lights, and the other carboxyl groups could further react with E51 at 120 °C. In the TIDC system, the thermal initiator triggered the polymerization of C═C at 120 °C and also its carboxyl groups can react with epoxy groups. The PTIDC and TIDC systems contained more reactive groups, which can build polymerized network systems with higher cross-linking density. For C═C groups, compared with thermal triggering polymerization, the UV triggering possess more polymerizing capability; thus, the PTIDC had the highest tensile strength of 32.71 MPa. The tensile testing results show that the dual-cross-linking process

https://doi.org/10.1021/acsomega.1c02199
ACS Omega 2021, 6, 21915−21924

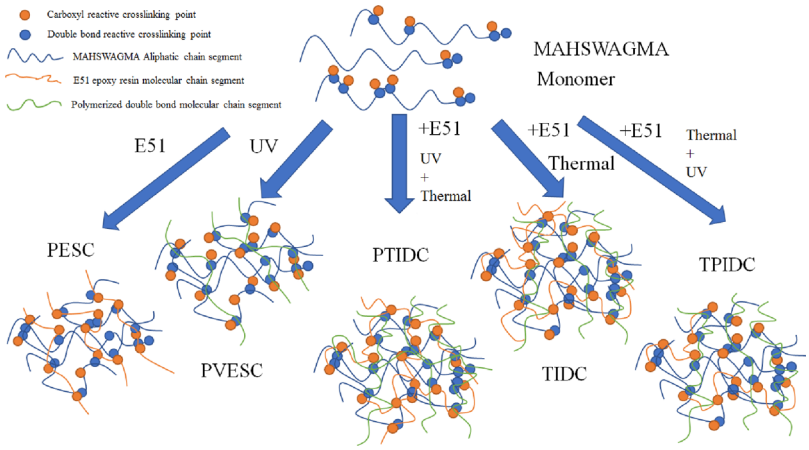

Figure 8. Formation schematic diagram of different cross-linking polymer network structures based on SWO with different preparation technologies.

can significantly improve the mechanical properties of polymer materials.

3.4. Morphology of the Different Copolymerized Systems. Figure 9 shows the scanning electron microscopy images of the tensile fracture surface of different specimens at a magnification of 500 times. The relatively smooth surface proves that all copolymers had formed excellent cross-linked structures. Images of PVESC and PESC showed plentiful scaly fragments and relatively rough surfaces, indicating their rapid brittle fractures. Nevertheless, in the three dual-cross-linking copolymers, the orderly strip tensile fracture surfaces were characteristic of elastomers, indicating that these three systems had excellent mechanical properties. Compared with these two single-cross-linking copolymers, the prepared three dual-cross-linking copolymers contained polymerized epoxy and vinyl ester cross-linking systems. Under the action of an external force, the molecular chain segments of the three dual-cross-linking copolymers were arranged regularly along the stretching direction. When the tension reached a certain value, the materials started to be torn along the weak parts of chemical bonds, which presented a more orderly banded structure.

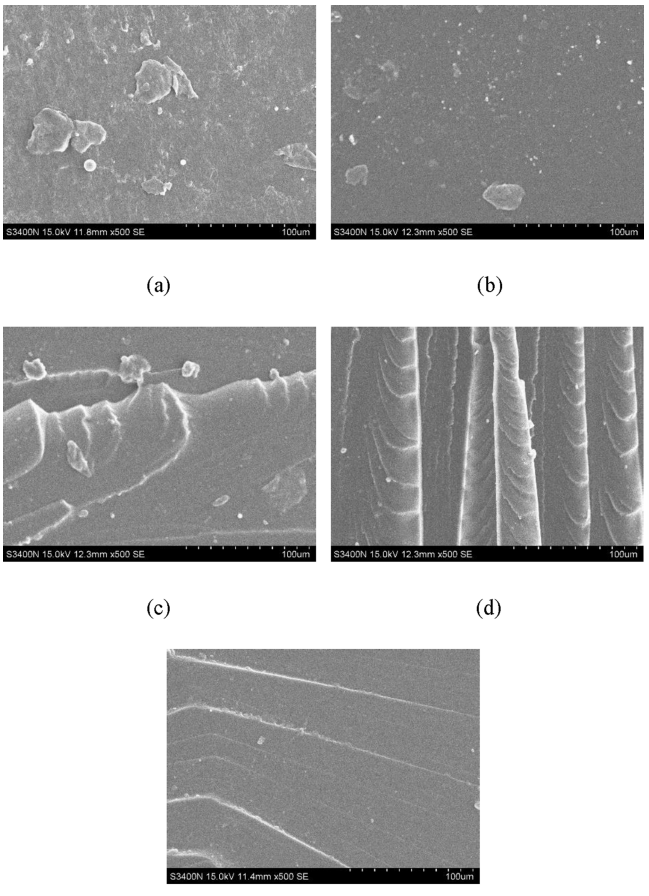

Figure 9. SEM images of tensile fracture surfaces of (a) PVESC, (b) PESC, (c) TPIDC, (d) PTIDC, and (e) TIDC.

3.5. DMA of Different Copolymers. The dynamic mechanical analysis curves of different copolymers are displayed in Figure 10. The rubber elasticity theory can be applied to calculate the cross-link density (ν_e). The relationship between cross-link density (ν_e) and storage modulus (E') is as follows:[30−32]

$$E' = 3\nu_e RT \quad (1)$$

where R is the gas constant and T is the absolute temperature (K). E' is referred to as the storage modulus at T_g + 30 °C. Table 3 shows the detailed ν_e data of copolymers from dynamic thermomechanical analysis. The tan δ curves of TPIDC and PTIDC display two different glass transition temperatures (T_g), and the relatively high temperature corresponding the high temperature peak was selected as the T_g of the copolymers.

The storage modulus (E') curves are shown in Figure 10a. As the temperature increases, all E' curves showed a similar downtrend: E' went down dramatically over a wide temperature range.

As shown in Figure 10a, E' curves remained at a high level above 2000 MPa. The copolymerized materials were in the glass state under −60 °C and all of the molecular segmental motions were frozen. The frozen segmental structures would relax suddenly with increase in temperature. E' values were also decreased rapidly and kept at a relative level below 200 MPa at above 70 °C.

E' of a copolymer is very sensitive to the cross-linking state and chemical structures of the copolymerized monomer. It is very similar to the macroscopical mechanical properties of the

https://doi.org/10.1021/acsomega.1c02199
ACS Omega 2021, 6, 21915−21924

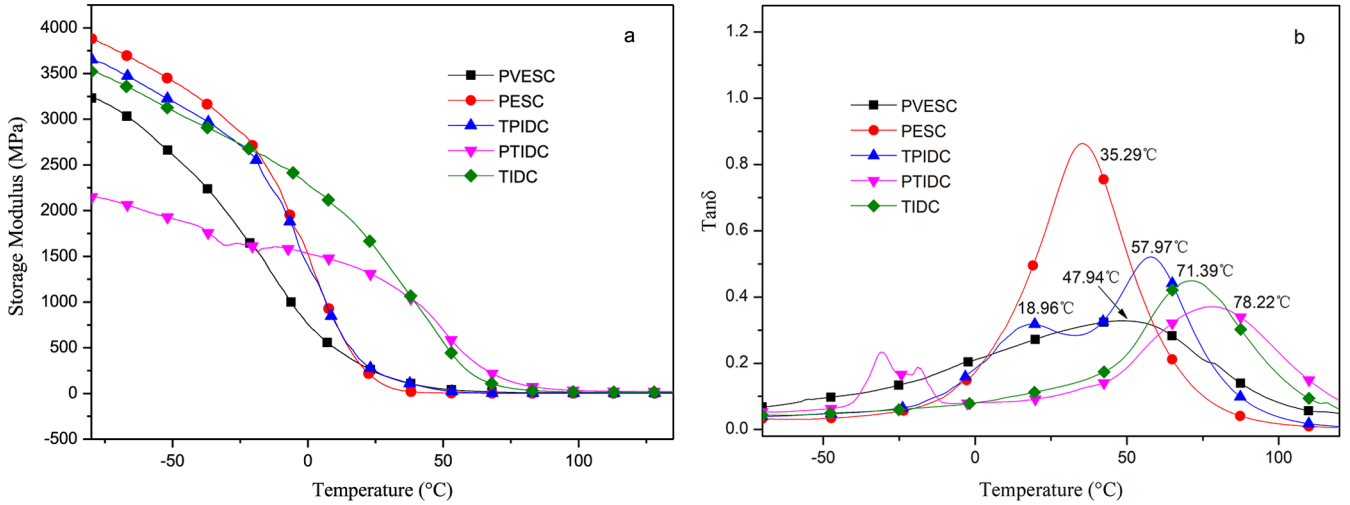

Figure 10. (a) Storage modulus (E') and (b) loss factor of the copolymers.

Table 3. ν_e of Different Copolymerized Systems

sample	T_g + 30 (K)	E' at T_g + 30 (MPa)	ν_e (mol·m^{-3})
PVESC	351.09	10.46	1193.97
PESC	338.44	2.94	349.08
TPIDC	361.12	3.50	388.58
PTIDC	381.37	25.60	2691.36
TIDC	374.54	16.11	1724.61

copolymer.[33,34] At low temperature (<−20 °C), E' of PESC remained a high level than others. The PESC copolymerized system possesses less cross-linking structures. The un-cross-linked segmental motions were easier to pile up tightly and form ordered structures, exhibiting strong cohesion. These effects endowed the PESC with a high energy storage modulus at low temperature. Although the E' values of the three dual-cross-linking copolymers at low temperature (<−20 °C) were lower than that of PESC, the downtrend of the E' curve of the two single-cross-linking polymers with the increase in temperature was more obvious compared with PTIDC and TIDC, indicating that the two dual-cross-linking polymers had higher heat resistance than the two single-cross-linking polymers.

Table 3 shows the ν_e of different copolymerized systems. As seen from Table 3, the ν_e of PTIDC and TIDC was higher than others. In PTIDC and TIDC, two functional groups, including carboxyl groups and double bond groups, can react with the epoxy groups. Thus, PTIDC and TIDC had a higher cross-link density than the two single-cross-linking copolymerized systems. However, the ν_e of TPIDC was low, which may be because the majority of the molecular segments were fixed after curing at 120 °C for 1 h and cannot move freely under UV light irradiation. Therefore, the ν_e of TPIDC is not ideal.

Figure 10b displays the loss factor (tan δ) curves of the copolymers. The tan δ curves of PVESC, PESC, and TIDC all display one T_g, indicating that the copolymerized systems were all in homogeneous cross-linking structures. However, the tan δ curves of TPIDC and PTIDC display two points of T_g, suggesting that the copolymerized systems contain relatively independent two types of cross-linking structures. For the TPIDC system, cured at 120 °C for 1 h, the carboxyl group reacted with the epoxy group in TPIDC to form the epoxy resin cross-linking system. Meanwhile, most of the molecular segments including C═C groups were fixed after curing and consequently cannot move freely for further polymerization,

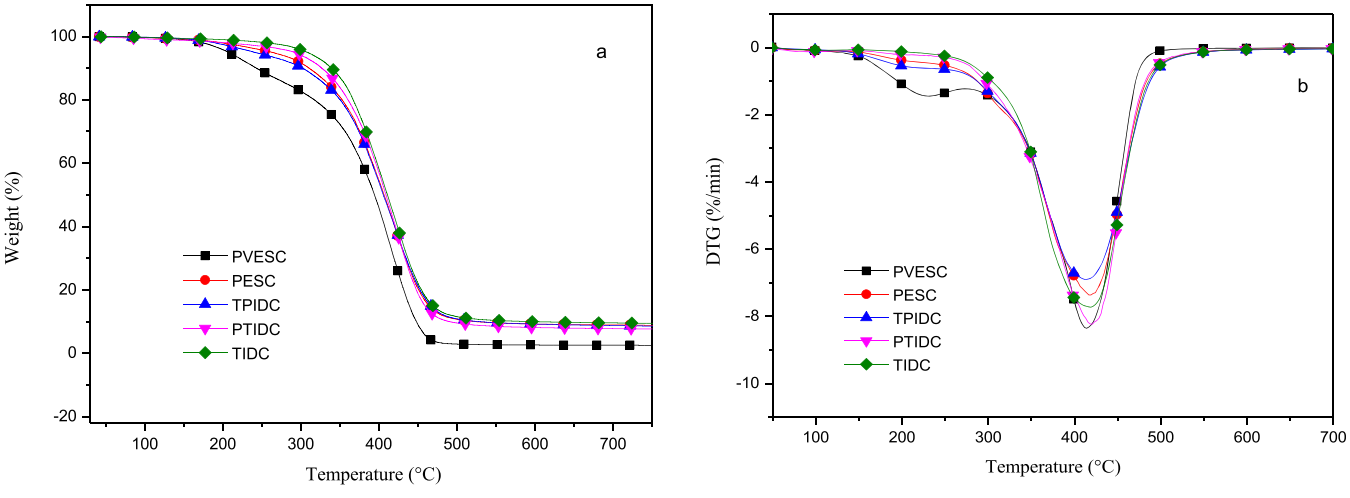

Figure 11. (a) TGA and (b) DTG curves of different copolymers.

https://doi.org/10.1021/acsomega.1c02199
ACS Omega 2021, 6, 21915−21924

and only a small number of double bonds were cross-linked to form the vinyl ester cross-linking network. Therefore, this copolymerized system consists of two independent cross-linking networks, and its tan δ curve displays two peaks. Moreover, the peak at low temperature corresponds to a kind of chain structure, which leads to the low cross-linking density of TPIDC. For PTIDC, the vinyl ester cross-linking network was generated under UV light irradiation; meanwhile, the part of carboxyl groups might react with the epoxy groups of E51 under the influence of thermal effect of UV lights, and the other carboxyl groups could further react with E51 at 120 °C. Therefore, the system consists of two independent cross-linking networks, and its tan δ curve displays two peaks, and the peak at about 18.96 °C was attributed to the C═C cross-linking structure.

For TIDC, however, a homogeneous vinyl ester-epoxy dual-cross-linking structure was formed after curing at certain temperature, leading to one T_g. PTIDC had the highest T_g (78.22 °C), while PESC had the lowest (35.29 °C). In general, T_g depends on the chemical structure and cross-linked state of the monomers.[35] The dual-cross-linking copolymerized systems prepared with dual-initiated preparation technology contain more active functional groups and cross-linked structures, which account for the higher cross-link density and the less activity of motion units, leading to the T_g transition to higher temperature.

3.6. TGA of Different Copolymers. On the basis of thermogravimetric analysis, the curves in Figure 11 and the data in Table 4 show the thermal decomposition behaviors of copolymers in N_2.

Table 4. Main Thermal Degradation of Different Copolymers[a]

		first thermal event		second thermal event		
samples	IDT (°C)	OT (°C)	DPR (%·min^{-1})	OT (°C)	DPR (%·min^{-1})	weight residue (%)
PVESC	180.1	231.8	−1.44	414.2	−8.35	2.54
PESC	342.4	419.9	−7.38			8.74
TPIDC	339.8	412.4	−6.89			8.47
PTIDC	351.0	420.8	−8.23			7.53
TIDC	349.5	418.3	7.72			9.34

[a]Remarks: Initial decomposition temperature (IDT); onset temperature (OT); and degradation peak rate (DPR).

As shown Table 4, PVESC has two different thermal degradation stages with an initial decomposition temperature (IDT) of 180.1 °C, but the other systems have only one distinct thermal decomposition stage with the IDT above 330 °C. All copolymers have undergone significant thermal decomposition at high temperature, and almost no carbon remains. The carbon yields of all five copolymers are less than 9.50%.

The PVESC copolymer has relatively low IDT (180.1 °C), which is probably due to the single cross-linking system formed by double bonds. Lower cross-linked density led to its lower IDT. In addition, the nonterminal double bonds of MAHSWAGMA resulted in the generation of the steric effect in the cross-linking process, which also led to a decrease in the relative cross-linking density. However, the onset decomposition temperature of PESC is relatively higher (342.4 °C). PESC has better thermal stability due to the presence of the epoxy cross-linking system. These three dual-cross-linking systems all had high IDT (>330 °C), which was the highest in PTIDC (351.0 °C). When the samples were heated to 351 °C, the polymerized points copolymerized by epoxy and vinyl groups began to fracture. With the increase in the heating temperature, a strong thermal degradation reaction took place accompanied by obvious weight loss. The decomposition rate can maximize at 420.8 °C.

PESC has a higher weight residue than PVESC (Table 4), probably due to the introduction of epoxy groups. In addition, for the prepared three dual-cross-linking systems, TPIDC and PTIDC have a higher weight residue than PVESC. These two dual-cross-linking systems contained more excellent cross-linking structures including polymerized epoxy and vinyl resin systems. Therefore, compared with PVESC, the weight residue of TPIDC and PTIDC dual-cross-linking systems were all improved. In addition, compared with the polymerized vinyl resin system, the epoxy cross-linking system has more benefits for the formation of carbon residues. For the PESC system, all epoxy groups were well copolymerized; thus, the PESC copolymerized system has a relatively higher weight residue.

4. CONCLUSIONS

The MAHSWAGMA monomer was successfully synthesized from SWO. Five prepared copolymers, named PVESC, PESC, TPIDC, PTIDC, and TIDC, were designed and prepared from MAHSWAGMA. Compared with the prepared two single-cross-linking copolymers, the prepared three dual-cross-linking copolymers had higher cross-linking densities, hardness, glass transition temperatures, and better tensile properties. For the MAHSWAGMA monomer, photo first and thermal latter initiated dual-cross-linking preparation technology had optimal curing result. Thus, the PTIDC copolymer had superior tensile strength (32.71 MPa), higher glass transition temperature (78.22 °C), the highest cross-link density (2691.36 mol·m^{-3}), and the highest IDT (381.37 °C). The tensile fracture surface of copolymers is relatively glossy and smooth indicating the formation of excellent cross-linking systems. This research has great implications for the preparation of biomaterials with excellent properties and provides an interesting biobased platform to access new biomaterials with excellent mechanical properties and high cross-linking density.

AUTHOR INFORMATION

Corresponding Author

Shouhai Li − *Institute of Chemical Industry of Forestry Products, CFA, Nanjing 210042 Jiangsu Province, China; Key Laboratory of Biomass Energy and Material, Nanjing 210042 Jiangsu Province, China; Co-Innovation Center of Efficient Processing and Utilization of Forest Resources, Nanjing Forestry University, Nanjing 210042 Jiangsu Province, China; Key and Open Laboratory of Forest Chemical Engineering, SFA, Nanjing 210042 Jiangsu Province, China; National Engineering Laboratory for Biomass Chemical Utilization, Nanjing 210042 Jiangsu Province, China; Institute of Forest New Technology, CFA, Beijing 100091, China;* orcid.org/0000-0001-8735-3295; Email: lishouhai1979@163.com

Authors

Ruitong Liu − *Institute of Chemical Industry of Forestry Products, CFA, Nanjing 210042 Jiangsu Province, China; Key Laboratory of Biomass Energy and Material, Nanjing*

https://doi.org/10.1021/acsomega.1c02199
ACS Omega 2021, 6, 21915−21924

210042 Jiangsu Province, China; Co-Innovation Center of Efficient Processing and Utilization of Forest Resources, Nanjing Forestry University, Nanjing 210042 Jiangsu Province, China; Key and Open Laboratory of Forest Chemical Engineering, SFA, Nanjing 210042 Jiangsu Province, China; National Engineering Laboratory for Biomass Chemical Utilization, Nanjing 210042 Jiangsu Province, China

Jing Yi − *Institute of Chemical Industry of Forestry Products, CFA, Nanjing 210042 Jiangsu Province, China; Key Laboratory of Biomass Energy and Material, Nanjing 210042 Jiangsu Province, China; Co-Innovation Center of Efficient Processing and Utilization of Forest Resources, Nanjing Forestry University, Nanjing 210042 Jiangsu Province, China; Key and Open Laboratory of Forest Chemical Engineering, SFA, Nanjing 210042 Jiangsu Province, China; National Engineering Laboratory for Biomass Chemical Utilization, Nanjing 210042 Jiangsu Province, China*

Jianling Xia − *Institute of Chemical Industry of Forestry Products, CFA, Nanjing 210042 Jiangsu Province, China; Key Laboratory of Biomass Energy and Material, Nanjing 210042 Jiangsu Province, China; Co-Innovation Center of Efficient Processing and Utilization of Forest Resources, Nanjing Forestry University, Nanjing 210042 Jiangsu Province, China; Key and Open Laboratory of Forest Chemical Engineering, SFA, Nanjing 210042 Jiangsu Province, China; National Engineering Laboratory for Biomass Chemical Utilization, Nanjing 210042 Jiangsu Province, China; Institute of Forest New Technology, CFA, Beijing 100091, China*

Mei Li − *Institute of Chemical Industry of Forestry Products, CFA, Nanjing 210042 Jiangsu Province, China; Key Laboratory of Biomass Energy and Material, Nanjing 210042 Jiangsu Province, China; Co-Innovation Center of Efficient Processing and Utilization of Forest Resources, Nanjing Forestry University, Nanjing 210042 Jiangsu Province, China; Key and Open Laboratory of Forest Chemical Engineering, SFA, Nanjing 210042 Jiangsu Province, China; National Engineering Laboratory for Biomass Chemical Utilization, Nanjing 210042 Jiangsu Province, China; Institute of Forest New Technology, CFA, Beijing 100091, China*

Haiyang Ding − *Institute of Chemical Industry of Forestry Products, CFA, Nanjing 210042 Jiangsu Province, China; Key Laboratory of Biomass Energy and Material, Nanjing 210042 Jiangsu Province, China; Co-Innovation Center of Efficient Processing and Utilization of Forest Resources, Nanjing Forestry University, Nanjing 210042 Jiangsu Province, China; Key and Open Laboratory of Forest Chemical Engineering, SFA, Nanjing 210042 Jiangsu Province, China; National Engineering Laboratory for Biomass Chemical Utilization, Nanjing 210042 Jiangsu Province, China; Institute of Forest New Technology, CFA, Beijing 100091, China*

Lina Xu − *Institute of Chemical Industry of Forestry Products, CFA, Nanjing 210042 Jiangsu Province, China; Key Laboratory of Biomass Energy and Material, Nanjing 210042 Jiangsu Province, China; Co-Innovation Center of Efficient Processing and Utilization of Forest Resources, Nanjing Forestry University, Nanjing 210042 Jiangsu Province, China; Key and Open Laboratory of Forest Chemical Engineering, SFA, Nanjing 210042 Jiangsu Province, China; National Engineering Laboratory for Biomass Chemical Utilization, Nanjing 210042 Jiangsu Province, China; Institute of Forest New Technology, CFA, Beijing 100091, China*

Xiaohua Yang − *Institute of Chemical Industry of Forestry Products, CFA, Nanjing 210042 Jiangsu Province, China; Key Laboratory of Biomass Energy and Material, Nanjing 210042 Jiangsu Province, China; Co-Innovation Center of Efficient Processing and Utilization of Forest Resources, Nanjing Forestry University, Nanjing 210042 Jiangsu Province, China; Key and Open Laboratory of Forest Chemical Engineering, SFA, Nanjing 210042 Jiangsu Province, China; National Engineering Laboratory for Biomass Chemical Utilization, Nanjing 210042 Jiangsu Province, China; Institute of Forest New Technology, CFA, Beijing 100091, China*

Na Yao − *Institute of Chemical Industry of Forestry Products, CFA, Nanjing 210042 Jiangsu Province, China; Key Laboratory of Biomass Energy and Material, Nanjing 210042 Jiangsu Province, China; Co-Innovation Center of Efficient Processing and Utilization of Forest Resources, Nanjing Forestry University, Nanjing 210042 Jiangsu Province, China; Key and Open Laboratory of Forest Chemical Engineering, SFA, Nanjing 210042 Jiangsu Province, China; National Engineering Laboratory for Biomass Chemical Utilization, Nanjing 210042 Jiangsu Province, China; Institute of Forest New Technology, CFA, Beijing 100091, China*

Complete contact information is available at: https://pubs.acs.org/10.1021/acsomega.1c02199

Notes

The authors declare no competing financial interest.

■ ACKNOWLEDGMENTS

This work was supported by the Fundamental Research Funds of Institute of Forestry Hi-Tech, Chinese Academy of Forestry (CAFYBB2020SZ007) and National Natural Science Foundation of China (31971598).

■ REFERENCES

(1) Atabani, A. E.; César, A. D. S. Calophyllum inophyllum L. A prospective non-edible biodiesel feedstock. Study of biodiesel production, properties, fatty acid composition, blending and engine performance. *Renew. Sustain. Energy Rev.* **2014**, *37*, 644−655.

(2) Li, B.; Xu, B.; Cheng, S.; Zhang, X. Physical and Chemical Properties of Cornus Wilsoniana Seed Oil Microcapsules and Its Product. *J. Chin. Cereals Oils Assoc.* **2018**, *33*, 58−62.

(3) Wu, L.; Deng, W.; Zhang, Y.; Lin, J.; Deng, Z.; Zhang, L.; He, Z.; Wang, M. Research on diurnal variation of photosynthetic characteristics of Cornus wilsoniana clones during friuting season. *J. Cent. South Univ. For. Technol.* **2017**, *37*, 32−37.

(4) Fu, J.; Zhang, X. W.; Liu, K.; Li, Q. S.; Zhang, L. R.; Yang, X. H.; Zhang, Z. M.; Li, C. Z.; Luo, Y.; He, Z. X.; Zhu, H. L. Hypolipidemic activity in Sprague-Dawley rats and constituents of a novel natural vegetable oil from Cornus wilsoniana fruits. *J. Food Sci.* **2012**, *77*, H160−H169.

(5) Zhang, Z. C.; Huang, J. H.; Ye, D. Q.; Li, W. F.; He, Z.; Cheng, X. R. Nitrogen and Phosphorus Stoichiometry of Different Families of Cornus wilsoniana and Their Relationships to Nutrient Availability. *J. NW For. Univ.* **2016**, *31*, 53−58.

(6) Chen, Y. Z.; Jiang, L. J.; Chen, J. Z.; Liu, Q.; Zhang, L. H.; Liu, J.; Zhao, Z. W. Diversity Analysis of Main Agronomic Characters of

Different Cornus wilsoniana Clones. *Plant Divers. Resour.* **2014**, *36*, 755−762.
(7) Xiao, Z. H.; Jiang, W. W.; Lin, L.; Vittayapadung, S.; Zhang, A. H.; Li, C. Z. Catalytic Cracking of Cornus wisoniana Oil to Liquid Bio-Fuel Oil Using KF/CaO as a Solid Base Catalyst. *Appl. Mech. Mater.* **2013**, *477-478*, 1446−1451.
(8) Li, C.; Ma, J.; Xiao, Z.; Hector, S. B.; Liu, R.; Zuo, S.; Xie, X.; Zhang, A.; Wu, H.; Liu, Q. Catalytic cracking of Swida wilsoniana oil for hydrocarbon biofuel over Cu-modified ZSM-5 zeolite. *Fuel* **2018**, *218*, 59−66.
(9) Zhang, J.; Zhang, L.; Jia, L. Variables Affecting Biodiesel Production from Zanthoxylum bungeanum Seed Oil with High Free Fatty Acids. *Ind. Eng. Chem. Res.* **2012**, *51*, 3525−3530.
(10) Ding, R.; Zhong, S. A.; Li, N.; Yang, J. J. Transesterification of Swida wilsoniana oil with methanol to biodiesel catalyzed by Lipozyme TL IM in MgCl2-saturated solution. *J. Fuel Chem. Technol.* **2010**, *38*, 287−291.
(11) Li, Y.; Wang, X.; Chen, J.; Cai, N.; Zeng, H.; Qiao, Z.; Wang, X. A method for micropropagation of Cornus wilsoniana: An important biofuel plant. *Ind. Crops Prod.* **2015**, *76*, 49−54.
(12) Rösch, J.; Mülhaupt, R. Polymers from renewable resoureces: polyester resins and blends based upon anhydride-cured epoxidized soybean oil. *Polym. Bull.* **1993**, *31*, 679−685.
(13) Gerbase, A. E.; Petzhold, C. L.; Costa, A. P. O. Dynamic mechanical and thermal behavior of epoxy resins based on soybean oil. *J. Am. Oil Chem. Soc.* **2002**, *79*, 797−802.
(14) Lee, S. H.; You, R.; Yoon, Y. I.; Park, W. H. Preparation and characterization of acrylic pressure-sensitive adhesives based on UV and heat curing systems. *Int. J. Adhes. Adhes.* **2017**, *75*, 190−195.
(15) Bayramoğlu, G.; Kahraman, M. V.; Kayaman-Apohan, N.; Güngör, A. Synthesis and characterization of UV-curable dual hybrid oligomers based on epoxy acrylate containing pendant alkoxysilane groups. *Prog. Org. Coat.* **2006**, *57*, 50−55.
(16) Lee, S.-W.; Park, J.-W.; Park, C.-H.; Lim, D.-H.; Kim, H.-J.; Song, J.-Y.; Lee, J.-H. UV-curing and thermal stability of dual curable urethane epoxy adhesives for temporary bonding in 3D multi-chip package process. *Int. J. Adhes. Adhes.* **2013**, *44*, 138−143.
(17) Park, C.-H.; Lee, S.-W.; Park, J.-W.; Kim, H.-J. Preparation and characterization of dual curable adhesives containing epoxy and acrylate functionalities. *React. Funct. Polym.* **2013**, *73*, 641−646.
(18) Tanoue, N.; Koishi, Y.; Atsuta, M.; Matsumura, H. Properties of dual-curable luting composites polymerized with single and dual curing modes. *J. Oral Rehabil.* **2003**, *30*, 1015−1021.
(19) Chang, C.-J.; Tzeng, H.-Y. Preparation and properties of waterborne dual curable monomers and cured hybrid polymers for ink-jet applications. *Polymer* **2006**, *47*, 8536−8547.
(20) Park, S.; Hwang, J. W.; Kim, K. N.; Lee, G. S.; Nam, J. H.; Noh, S. M.; Jung, H. W. Rheology and curing characteristics of dual-curable clearcoats with hydroxyl functionalized urethane methacrylate oligomer: Effect of blocked isocyanate thermal crosslinkers. *Korea-Aust. Rheol. J.* **2014**, *26*, 159−167.
(21) Chang, R.; Qin, J.; Gao, J. RETRACTED ARTICLE: Fully biobased epoxy from isosorbide diglycidyl ether cured by biobased curing agents with enhanced properties. *J. Polym. Res.* **2014**, *21*, 501.
(22) Wan, J.; Gan, B.; Li, C.; Molina-Aldareguia, J.; Kalali, E. N.; Wang, X.; Wang, D.-Y. A sustainable, eugenol-derived epoxy resin with high biobased content, modulus, hardness and low flammability: Synthesis, curing kinetics and structure−property relationship. *Chem. Eng. J.* **2016**, *284*, 1080−1093.
(23) Xie, C.; Zeng, B.; Gao, H.; Xu, Y.; Luo, W.; Liu, X.; Dai, L. Improving thermal and flame-retardant properties of epoxy resins by a novel reactive phosphorous-containing curing agent. *Polym. Eng. Sci.* **2014**, *54*, 1192−1200.
(24) Chiari, L.; Zecca, A. Constraints of fossil fuels depletion on global warming projections. *Energy Policy* **2011**, *39*, 5026−5034.
(25) Shafiee, S.; Topal, E. When will fossil fuel reserves be diminished? *Energy Policy* **2009**, *37*, 181−189.
(26) Hoel, M.; Kverndokk, S. Depletion of fossil fuels and the impacts of global warming. *Resour. Energy Econ.* **1996**, *18*, 115−136.
(27) Bryan, B. A.; Ward, J.; Hobbs, T. An assessment of the economic and environmental potential of biomass production in an agricultural region. *Land Use Policy* **2008**, *25*, 533−549.
(28) Welfle, A.; Gilbert, P.; Thornley, P. Increasing biomass resource availability through supply chain analysis. *Biomass Bioenergy* **2014**, *70*, 249−266.
(29) Tan, Z.; Chen, K.; Liu, P. Possibilities and challenges of China's forestry biomass resource utilization. *Renew. Sustain. Energy Rev.* **2015**, *41*, 368−378.
(30) Asif, A.; Shi, W.; Shen, X.; Nie, K. Physical and thermal properties of UV curable waterborne polyurethane dispersions incorporating hyperbranched aliphatic polyester of varying generation number. *Polymer* **2005**, *46*, 11066−11078.
(31) Liu, C.; Lei, W.; Cai, Z.; Chen, J.; Hu, L.; Dai, Y.; Zhou, Y. Use of tung oil as a reactive toughening agent in dicyclopentadiene-terminated unsaturated polyester resins. *Ind. Crops Prod.* **2013**, *49*, 412−418.
(32) Lu, J.; Khot, S.; Wool, R. P. New sheet molding compound resins from soybean oil. I. Synthesis and characterization. *Polymer* **2005**, *46*, 71−80.
(33) La Scala, J. J.; Ulven, C. A.; Orlicki, J. A.; Jain, R.; Palmese, G. R.; Vaidya, U. K.; Sands, J. M. Emission modeling of styrene from vinyl ester resins. *Clean Technol. Environ. Policy* **2007**, *9*, 265−279.
(34) Li, S.; Xia, J.; Li, M.; Huang, K. New Vinyl Ester Biocopolymers Derived from Dimer Fatty Acids: Preparation, Characterization and Properties. *J. Am. Oil Chem. Soc.* **2013**, *90*, 695−706.
(35) Wang, S.; Wang, J.; Ji, Q.; Shultz, A. R.; Ward, T. C.; McGrath, J. E. Miscibility and morphologies of poly(arylene ether phenyl phosphine oxide/sulfone) copolymer/vinyl ester resin mixtures and their cured networks. *J. Polym. Sci., Part B: Polym. Phys.* **2000**, *38*, 2409−2421.

https://doi.org/10.1021/acsomega.1c02199
ACS Omega 2021, 6, 21915−21924